Highly stable, 54mJ Yb-InnoSlab laser platform at 0.5kW average power

Journal Article

Author(s):
Schmidt, Bruno E.; Hage, Arvid; Mans, Torsten; Légaré, François; Wörner, Hans Jakob

Check for updates

Highly stable, 54mJ Yb-InnoSlab laser platform at 0.5kW average power

Bruno E. Schmidt,[1,*] Arvid Hage,[2] Torsten Mans,[2] François Légaré,[3] and Hans Jakob Wörner[4]

[1] few-cycle Inc., 2890 rue de Beaurivage, Montréal, H1L 5W5, QC, Canada
[2] Amphos GmbH, Kaiserstraße 100, 52134 Herzogenrath, Germany
[3] INRS-EMT, 1650 Blvd. Lionel Boulet, J3X 1S2, Varennes, Canada
[4] ETH – Zürich, Vladimir-Prelog-Weg 2, 8093 Zürich, Switzerland
*schmidt@few-cycle.com

Abstract: We report on the leap of Yb-InnoSlab laser technology towards high pulse energies of 54mJ combined with high average power exceeding half a kW. The system features pulse durations of 1.5 picoseconds (ps) at 10kHz repetition rate with excellent beam properties (M^2 of 1.1) combined with superb power and pointing stability in the sub-% range. It provides different output ports to facilitate optical synchronization for pumping parametric amplifiers. Tunable, femtosecond seed pulses are derived directly from the ps Yb pump pulses. We investigate the long term stability of this ps driven white light continuum and demonstrate 100-fold pulse compression down to 10fs duration. Ultra-broadband IR spectra centred at 2µm wavelength are subsequently generated via difference frequency generation of selected white light components.

References and links

1. J. Meijer, K. Du, A. Gillner, D. Hoffmann, V. S. Kovalenko, T. Masuzawa, A. Ostendorf, R. Poprawe, and W. Schulz, "Laser machining by short and ultrashort pulses, state of the art and new opportunities in the age of the photons," Ann. Manuf. Technol. **51**(2), 531–550 (2002).
2. A. Dubietis, R. Butkus, and A. P. Piskarskas, "Trends in chirped pulse optical parametric amplification," IEEE J. Sel. Top. Quantum Electron. **12**(2), 163–172 (2006).
3. G. Cerullo and S. De Silvestri, "Ultrafast optical parametric amplifiers," Rev. Sci. Instrum. **74**(1), 1–18 (2003).
4. I. Will and G. Klemz, "Generation of flat-top picosecond pulses by coherent pulse stacking in a multicrystal birefringent filter," Opt. Express **16**(19), 14922–14937 (2008).
5. B. A. Reagan, M. Berrill, K. A. Wernsing, C. Baumgarten, M. Woolston, and J. J. Rocca, "High-average-power, 100-Hz-repetition-rate, tabletop soft-x-ray lasers at sub-15-nm wavelengths," Phys. Rev. A **89**(5), 053820 (2014).
6. http://cymer.com/euv-light-sources/
7. A. N. Bashkatov, E. A. Genina, V. I. Kochubey, and V. V. Tuchin, "Optical properties of human skin, subcutaneous and mucous tissues in the wavelength range from 400 to 2000 nm," J. Phys. D Appl. Phys. **38**(15), 2543–2555 (2005).
8. Y. K. Yap, M. Inagaki, S. Nakajima, Y. Mori, and T. Sasaki, "High-power fourth- and fifth-harmonic generation of a Nd:YAG laser by means of a CsLiB6O10," Opt. Lett. **21**(17), 1348–1350 (1996).
9. B. E. Schmidt, N. Thiré, M. Boivin, A. Laramée, F. Poitras, G. Lebrun, T. Ozaki, H. Ibrahim, and F. Légaré, "Frequency domain optical parametric amplification," Nat. Commun. **5**, 3643 (2014).
10. S. Witte and K. S. E. Eikema, "Ultrafast optical parametric chirped-pulse amplification," IEEE J. Sel. Top. Quantum Electron. **18**(1), 296–307 (2012).
11. S.-W. Huang, J. Moses, and F. X. Kärtner, "Broadband noncollinear optical parametric amplification without angularly dispersed idler," Opt. Lett. **37**(14), 2796–2798 (2012).
12. A. Thai, M. Hemmer, P. K. Bates, O. Chalus, and J. Biegert, "Sub-250-mrad, passively carrier-envelope-phase-stable mid-infrared OPCPA source at high repetition rate," Opt. Lett. **36**(19), 3918–3920 (2011).
13. N. Ishii, K. Kaneshima, K. Kitano, T. Kanai, S. Watanabe, and J. Itatani, "Sub-two-cycle, carrier-envelope phase-stable, intense optical pulses at 1.6 µm from a BiB3O6 optical parametric chirped-pulse amplifier," Opt. Lett. **37**(20), 4182–4184 (2012).

14. J. Novák, J. T. Green, T. Metzger, T. Mazanec, B. Himmel, M. Horáček, Z. Hubka, R. Boge, R. Antipenkov, F. Batysta, J. A. Naylon, P. Bakule, and B. Rus, "Thin disk amplifier-based 40 mJ, 1 kHz, picosecond laser at 515 nm," Opt. Express **24**(6), 5728–5733 (2016).

15. S. Klingebiel, M. Schultze, C. Y. Teisset, R. Bessing, M. Haefner, S. Prinz, M. Gorjan, D. H. Sutter, K. Michel, H. G. Barros, Z. Major, F. Krausz, and T. Metzger, "220mJ ultrafast thin-disk regenerative amplifier", in *CLEO: 2015*, OSA Technical Digest (Online) (Optical Society of America, 2015), p. STu4O.2.

16. J. P. Negel, A. Loescher, A. Voss, D. Bauer, D. Sutter, A. Killi, M. A. Ahmed, and T. Graf, "Ultrafast thin-disk multipass laser amplifier delivering 1.4 kW (4.7 mJ, 1030 nm) average power converted to 820 W at 515 nm and 234 W at 343 nm," Opt. Express **23**(16), 21064–21077 (2015).

17. E. Kaksis, G. Andriukaitis, T. Floery, A. Pugzlys, and A. Baltuska, "30-mJ 200-fs cw-pumped Yb:CaF2 regenerative amplifier", in *Conference on Lasers and Electro-Optics*, OSA Technical Digest (2016) (Optical Society of America, 2016), p. STh4J.6.

18. C.-L. Chang, P. Krogen, K.-H. Hong, L. E. Zapata, J. Moses, A.-L. Calendron, H. Liang, C.-J. Lai, G. J. Stein, P. D. Keathley, G. Laurent, and F. X. Kärtner, "High-energy, kHz, picosecond hybrid Yb-doped chirped-pulse amplifier," Opt. Express **23**(8), 10132–10144 (2015).

19. C. Baumgarten, M. Pedicone, H. Bravo, H. Wang, L. Yin, C. S. Menoni, J. J. Rocca, and B. A. Reagan, "1 J, 0.5 kHz repetition rate picosecond laser," Opt. Lett. **41**(14), 3339–3342 (2016).

20. M. Kienel, M. Müller, A. Klenke, J. Limpert, and A. Tünnermann, "12 mJ kW-class ultrafast fiber laser system using multidimensional coherent pulse addition," Opt. Lett. **41**(14), 3343–3346 (2016).

21. P. Russbueldt, T. Mans, J. Weitenberg, H. D. Hoffmann, and R. Poprawe, "Compact diode-pumped 1.1 kW Yb:YAG Innoslab femtosecond amplifier," Opt. Lett. **35**(24), 4169–4171 (2010).

22. M. Kellert, M. Pergament, K. Kruse, J. Wang, G. Palmer, G. Priebe, L. Wissmann, U. Wegner, M. Emons, J. Morgenweg, T. Mans, and M. J. Lederer, "5kW burst-mode femtosecond amplifier system for the European XFEL pump-probe laser development", in 2015 European Conference on Lasers and Electro-Optics - European Quantum Electronics Conference (OSA, 2015), paper CA_3_5.

23. A. Baltuška, T. Fuji, and T. Kobayashi, "Controlling the carrier-envelope phase of ultrashort light pulses with optical parametric amplifiers," Phys. Rev. Lett. **88**(13), 133901 (2002).

24. P. Russbueldt, T. Mans, G. Rotarius, J. Weitenberg, H. D. Hoffmann, and R. Poprawe, "400W Yb:YAG Innoslab fs-amplifier," Opt. Express **17**(15), 12230–12245 (2009).

25. M. Rumpel, M. Moeller, C. Moormann, T. Graf, and M. A. Ahmed, "Broadband pulse compression gratings with measured 99.7% diffraction efficiency," Opt. Lett. **39**(2), 323–326 (2014).

26. M. Bradler, P. Baum, and E. Riedle, "Femtosecond continuum generation in bulk laser host materials with sub-µJ pump pulses," Appl. Phys. B **97**(3), 561–574 (2009).

27. A.-L. Calendron, H. Çankaya, G. Cirmi, and F. X. Kärtner, "White-light generation with sub-ps pulses," Opt. Express **23**(11), 13866–13879 (2015).

28. J. Galinis, G. Tamošauskas, I. Gražulevičiūtė, E. Keblytė, V. Jukna, and A. Dubietis, "Filamentation and supercontinuum generation in solid-state dielectric media with picosecond laser pulses," Phys. Rev. A **92**(3), 033857 (2015).

29. R. Riedel, A. Stephanides, M. J. Prandolini, B. Gronloh, B. Jungbluth, T. Mans, and F. Tavella, "Power scaling of supercontinuum seeded megahertz-repetition rate optical parametric chirped pulse amplifiers," Opt. Lett. **39**(6), 1422–1424 (2014).

30. G. Ernotte, P. Lassonde, F. Légaré, and B. E. Schmidt, "Frequency domain tailoring for intra-pulse frequency mixing," Opt. Express **24**(21), 24225–24231 (2016).

31. P. Lassónde, N. Thiré, L. Arissian, G. Ernotte, F. Poitras, T. Ozaki, A. Laramée, M. Boivin, H. Ibrahim, F. Légaré, and B. E. Schmidt, "High gain frequency domain optical parametric amplification," IEEE J. Sel. Top. Quantum Electron. **21**(5), 8700410 (2015).

32. J. Rothhardt, S. Demmler, S. Hädrich, T. Peschel, J. Limpert, and A. Tünnermann, "Thermal effects in high average power optical parametric amplifiers," Opt. Lett. **38**(5), 763–765 (2013).

1. Introduction

High average power lasers delivering short pulses on the order of few picosecond (ps) durations are among the most up-and-coming technologies in contemporary laser science. Applications include industrial manufacturing [1], pumping of optical parametric chirped pulse amplifiers (OPCPAs) [2,3], photo injector lasers for free electron lasers [4], or as a direct pump source for XUV lasers [5] to name but a few.

While gas lasers like the industry workhorse CO_2 are capable of delivering multi-Joules of pulse energies and operation in extraordinary average power regimes up to 30kW [6], their typical pulse duration in the nanosecond range and far infrared wavelength of 10µm set limits for many applications. A strategically very good wavelength is 1µm. It lies in the transparency range where many optical materials have minimum absorption or scattering and it enables high penetration depth in human tissues [7]. A variety of solid-state gain media

around 1μm wavelength can be resourcefully pumped by near-infrared (NIR) laser diodes and these media even support sub-ps pulse durations. The few-ps duration is optimal to keep the laser induced damage thresholds at the highest level, which allows to drive nonlinear processes at high intensities. Furthermore, 1 μm lasers can be efficiently frequency shifted up to their fifth har-monic [8] and can pump OPAs in the IR range [9–13], presumably at very high average power.

Therefore, Yb-doped laser crystals exhibiting a very low quantum defect of ~9% in combination with the relatively high thermal conductivity of the Yttrium Aluminium Garnet (YAG) host (14W/mK) became the most popular material for high peak and average power laser with ps duration. The current state of the art of alternative concepts comprises:

- water cooled thin disks (90W, 90mJ, 1kHz, 1.2ps [14]; 220W, 220mJ, 1kHz, 1.9ps [15], 1.4kW, 4.7mJ, 300kHz, 6.5ps [16]),

- cryogenically cooled rods (15W, 30mJ, 0.5kHz, 0.2ps [17]; 70W, 70mJ, 1kHz, 6ps [18]; 500W, 1J, 0.5kHz, 5ps [19]),

- coherent addition of water cooled fiber rods (700W, 12mJ, 58kHz, 0.26ps [20]).

For the InnoSlab laser concept, average powers of 1.1kW (20MHz, 615fs, 55μJ) [21] and single pulse energies of 43mJ (burst-mode 10Hz repetition rate, average power approximately 26W, net burst duration 600μs, intra-burst repetition rate 100kHz, 800fs) [22] have been reported. In this contribution, we report on the boosting of the InnoSlab technology to 540W of average power associated with a pulse energy of 54mJ at 10kHz repetition rate and 1.5ps pulse duration. This is a significant enhancement in terms of pulse energy (100 times) compared to [21] and average power (20 times) compared to [22]. We characterize the system in terms of pulse energy, beam pointing stability as well as spatial beam quality. Furthermore, we demonstrate 100 fold pulse compression of the ps driven white light (WL) down to about 10fs duration with conventional reflection gratings. We use these compressed visible (VIS) pulses as the pump pulse in a subsequent difference frequency generation (DFG) process to reach ultra-broadband IR pulses at 2μm wavelength. This DFG output is expected to be passively carrier envelope phase (CEP) stabilized [23].

2. Laser layout

Since bare pump power without fidelity is hardly beneficial to drive nonlinear optics, substantial engineering efforts were made to provide state of the art spatio-temporal beam
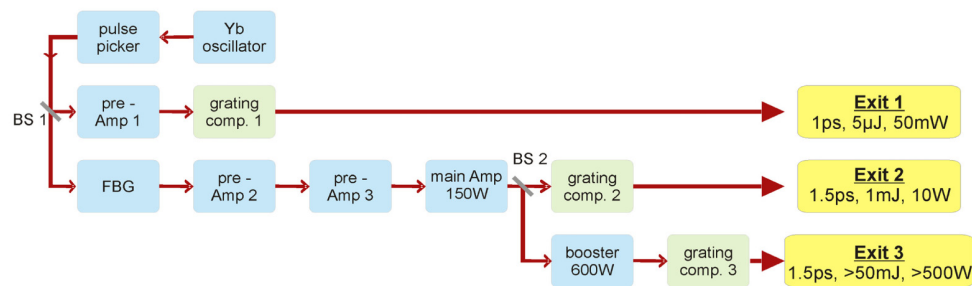

Fig. 1. Schematic diagram of the Yb-InnoSlab platform providing three different exit ports at different power levels, all derived from the same oscillator pulse to minimize temporal jitter. The total optical path between exit 1 to exit 3 is only about 16m. BS: beam splitter, FBG: fiber Bragg grating, comp: compressor, Amp: amplifier.

quality paired with excellent stability. Another crucial aspect for pumping parametric amplifiers is the timing synchronization between seed and pump pulses. To facilitate optical synchronization, the Yb InnoSlab platform (sketched in Fig. 1) offers three different optical

outputs at different power levels (yellow in Fig. 1). All outputs are derived from the same oscillator pulse to avoid the necessity of stabilizing the oscillator repetition rate. The seed is generated in a fiber oscillator operating at 20MHz repetition rate with pulse energy around 1nJ. A subsequent pulse picker enables variation of the repetition rate from 2MHz down to 10kHz while maintaining the same average power on all three exit ports. Prior to the first beam splitter BS 1, the pulse energy is raised with conventional fiber amplifiers to 50nJ.

Exit 1 is obtained from the beam transmitted at BS 1 which is amplified unstretched in an Yb rod amplifier (pre-Amp 1) to the multi µJ level. The material dispersion acquired in this arm is compensated with a small grating compressor to deliver 1ps pulses carrying 5µJ of energy at 10kHz repetition rate. With a grating separation of approximately 40mm and a grove density of 1600 lines/mm-grating in Littrow configuration a GVD of approximately + 1.23ps^2 is removed. The total footprint of this compressor is about 15cm x 15cm.

For the high average power arms, the beam reflected at BS 1 is temporally stretched with a fiber Bragg grating (FBG) to ~250ps and subsequently amplified in a fiber amplifier followed by Yb rod amplifiers (pre-Amp 2 & 3) to a pulse energy of 100µJ. After beam expansion, it is further amplified in the main amplifier based on the InnoSlab approach. Details of laser crystal and pump geometry of this first InnosSlab amplifier stage are described in [24], with the difference that the number of passes has been changed from 9 to 7; crystal dimensions stayed at 10mm x 10mm x 1mm and the pumping intensities falling on the crystal facets are exceeding 25kW/cm^2 to reach the desired amplification regime. Here, the pulses reach the 15mJ level corresponding to 150W of average power. The optical to optical efficiency of this main amplifier pumped by 940nm cw diodes is about 28%. To maximize the reliability and stability of the entire system, this stage is operated below its maximum power level: to reach 150W of average power at 1030nm, the current of the pump diodes is about 50% below its nominal value. A design at such low pump diode current was chosen to provide maintenance free operation over a long term, presumably for many years. At an elevated diode current, this main amplifier could deliver >400W of average power at an increased repetition rate of >30kHz to keep the pulse energy constant. Another feature of the system is its compactness. All components, from the oscillator up to the main amplifier, are embedded in a sealed housing with a footprint of 0.7m x 1.1m.

Following the main amplifier, a second variable beam splitter (BS 2) consisting of a half wave plate and polarizing cube splits off about 10% to provide an intermediate output, labeled exit 2 in Fig. 1. This optional output might be useful when the system is used to pump a parametric amplifier chain that requires pumping at different energy levels. The RMS value for its power stability measured over 170 minutes is 0.22% and the pointing stability is 0.1% of the beam diameter in both directions (data not shown). These stability values are remarkably good, especially for a 150W ps laser with 15mJ pulse energy.

The transmitted 90% subsequent to BS 2 are sent to the booster amplifier. The basic architecture of this amplifier stage is comparable to the one in [21], but with two important changes: First, the crystal-width has been scaled to 25mm and the cw pump power has been scaled to an average of up to 2.7kW. Secondly, it has been turned to a 2-pass amplifier by back folding the beam through the crystal and separation via polarization rotation and a thin film polarizer. It raises the average power beyond 630W at 10kHz repetition rate. This output power is reached including an optical isolator at the booster exit, which is based on a slab design and reaches a transmission efficiency of about 95%. The optical efficiency of the booster is around 23% when the diodes are powered with 170A, which is 18% below their nominal value. The total wall-plug efficiency of the whole laser is estimated to be 5.8%.

The pulses are compressed with a grating compressor consisting of two multilayer dielectric gratings [25] with a total transmission of 86%. The compressor is very compact due to the small grating sizes of 20mm and 100mm, respectively and the folded beam path between the gratings, separated by 1.3m. At a higher repetition rate, meaning at lower peak power, the average power of this booster design could be increased up to 1.5kW with the

implemented hardware. We anticipate that the grating dimensions at the kW level will remain similar. The size of the booster amplifier and the grating compressor for the 500W output are both 0.7m x 1.1m, like the main amplifier. Thus, the footprint of the total system is about 2.4m x 1.1m.

3. Results and discussion
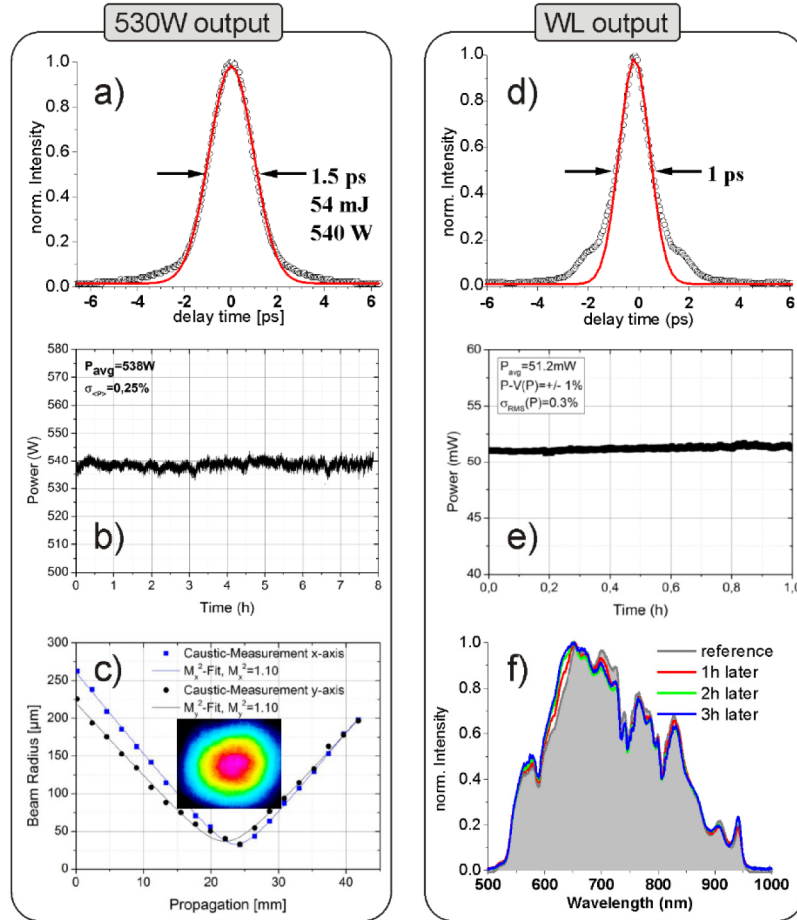

Fig. 2. Characterization of exit 3 in (a-c) and exit 1 in (d-f).(a) 1.5ps, close to transform limited pulses can be reached after compression 540W output. (b) The power stability after compression at 540W measured over 8h of operation is excellent with an RMS value of only 0.25%. (c) A round beam profile (inset) with an excellent M^2 value of 1.1 is obtained. (d) 1ps, 5µJ pulses are obtained after compression on exit 1. (e) The power stability measured over 1h shows a standard deviation of 0.3%. (f) This power stability is maintained upon white light generation in YAG. It was characterized over 3h of operation. More details are given in the text.

The measured autocorrelation for exit 3 after compressing the 540W output is shown in Fig. 2(a) as the black curve (APE pulse check). The Gaussian fit shown in red denotes a deconvolved FWHM pulse duration of 1.56ps which is very close to the transform limit of 1.42ps. The spatial properties depicted in Fig. 2(c) show an excellent M^2 of 1.1 in both directions together with a smooth and symmetric near filed beam profile in the inset. The transform limited beam properties, both in time and space, suggest a low amount of nonlinear distortions of the entire amplification chain up to the 0.5kW level of average power at a pulse power of 34GW. The long term average power stability measurement of the 540W beam

shown in Fig. 2(b) was carried out over 8h with a water-cooled power meter (Coherent PM5000). The extremely low RMS noise level of 0.25% is probably limited by the noise performance of the detector and by the back water cooling stability. Beam pointing measurement have been carried out as well (Basler AC1280 camera) behind compressor 3 over 4h. The RMS value for the pointing stability is 0.5% and 1.8% of the beam diameter in the horizontal and vertical direction, respectively (data not shown).

Parasitic oscillations could, in principle, occur [23], but as the overall amplification is lower compared to [23], we did not observe this effect in the present system. To prevent this effect further, every amplifier is terminated with specially developed faraday isolators providing 28-30dB isolation between every stage. For the 2-pass booster-amplifier, the net amplification is too low to give rise to parasitic oscillations. Depletion of the inversion due to ASE has not yet been observed in any of the described Yb-based InnoSlab laser setups so far.

Of paramount importance for the performance of the entire parametric amplifier chain is the seed generation which is derived from exit 1. The results in Fig. 2(d) show a Gaussian fit (red curve) to the experimental autocorrelation (black curve) with a deconvolved FWHM pulse duration of 1.03ps. A small pedestal at the 15% level is visible. The output energy after compression is 5µJ; it also exhibits an excellent stability of 0.3% RMS measured over 1h (Thorlabs PM100D), see Fig. 2(e). Since this output is used for the seed generation via super-continuum generation in a YAG crystal, we investigated the long term performance of the white light (WL) generation. More details about ps WL generation in general can be found in [26–29]. Typical WL spectra at 20kHz repetition rate obtained with about 2-3µJ of pulse energy are shown in Fig. 2(f). The spectra are taken after transmitting through a high reflecting mirror at 1030nm (Ocean Optics USB4H05240). The different curves, taken over a period of 3 hours at hourly intervals, show virtually no difference. To investigate the WL stability more thoroughly, a series of 1000 spectra was acquired at each hour. The shortest possible spectrometer integration time is 3.8ms, which corresponds to a seventy-six fold average. Each measurement was integrated in the spectral region from 500 to 1000nm for which an RMS value was evaluated. Over a time period of 3 hours, the RMS noise of the integrated WL power varied between 0.1% and 0.3%. This WL stability corresponds to the one of the ps input pulses and it is also excellent.

After characterizing the WL stability, the next steps were to investigate the ability to compress the super-continuum and to select different parts for DFG. Note that the spectral components around the fundamental and beyond are not detected with our experimental arrangement. To tailor the DFG input, we utilized a folded 4f arrangement as an "all inline pump-probe setup" which is explained in detail in [30]. It enables simultaneously: (i) pulse compression, (ii) spectral selection of wavelengths for subsequent DFG, (iii) delay adjustment between pump and signal wavelengths and (iv) potentially polarization control of spectral
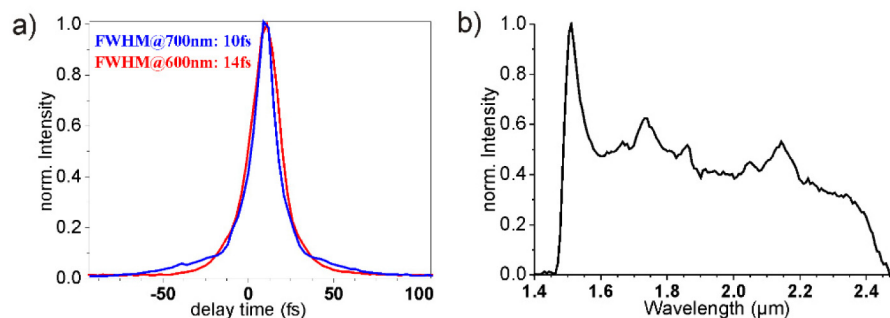

Fig. 3. WL compression and DFG. (a) Spectral parts around 700nm and 600nm are compressed to 10fs (blue curve) and 14fs (red curve), respectively, with a simple grating setup. (b) Spectral components around 620nm are mixed with light at 900nm to yield the DFG output in centered at 1.95µm.

components. The 4f setup had a transmission of about 50% for the WL and delivered about 1-2nJ of pulse energy in this spectral region. We selected the spectral regions around 700nm and 600nm, respectively, to perform grating based pulse compression. The results in Fig. 3(a) show an autocorrelation at 700nm with a deconvolved FWHM duration of 10fs (blue curve) and 14fs at 600nm, respectively. Since the grating position in the 4f setup that defines the amount of negative chirp is different in both cases, we conclude that the WL exhibits a strong (higher order) chirp. Our simple compression approach does not offer higher order chirp compensation and the wings in the autocorrelation (Fig. 3(a)) indicate the presence of third order dispersion. Nevertheless, if a 14fs pulse is used as the pump pulse in a DFG process, a similar pulse duration should be possible for the DFG output.

Consequently, we mixed the 14fs pulses around 620nm with a narrowband spectral slice of 10nm centred around 900nm in a periodically poled lithium niobate (PPLN) crystal with a poling period of 11.5μm. The resulting DFG spectrum is shown in Fig. 3(b). Broadband IR spectra are obtained spanning from 1.45 to at least 2.45μm, which is the limit of the IR spectrometer (Ocean Optics NIR 256). Although the DFG energy was too low to measure the pulse energy or an autocorrelation with the available equipment, the 1000nm bandwidth at 1.9μm center wavelength suggests that all pump wavelengths contribute to the DFG process. The estimated Fourier limit of this IR spectrum is about 14fs (corresponding to 2 optical cycles) which is equal to the duration of the pump pulses.

The ultimate goal is to amplify the IR pulses with multiple Fourier plane optical parametric amplifier (FOPA) stages [9]. While the design of the first, high gain stages may benefit from previous developments [31], the final FOPA stage, pumped at the half kW level at 10kHz repetition rate, denotes a venture into an uncharted terrain. Recently, Rothhardt et al. have identified severe average power limitations of OPCPA pumping at the 100W level [32]. The main issue is thermal gradients across the nonlinear crystal stemming from the round pump beam profile. However, in the Fourier plane of a FOPA the pump and seed beams are stretched out in one dimension to form a line. This rectangular aperture shape, potentially with an aspect ratio of 10/1, denotes a much more favorable surface to volume ratio for thermal management as compared to the symmetric case in a conventional OPCPA. In other words, a FOPA can be viewed as the parametric equivalent to the Innoslab approach. Our contribution to this point is the demonstration that this concept is capable of extremely stable operation at the half kW level of average power with 54mJ of pulse energy at 10kHz repetition rate with a very short pulse duration of 1.5ps. We also show that white light generation driven with such ps pulses is very stable and it enables 100 fold pulse compression with a simple grating compressor.

Funding